


Dynamics study of the operating behavior of hydrodynamic coupling by experimental and numerical simulation

T. Khatir*, M. Bouchetara**, D. Boutchicha***

*University of Science and Technology of Oran Mohammed Boudiaf, L.P 1505 EL-Menaour, USTO 31000 Oran, Algeria, E-mail: khatir-usto@hotmail.fr

**University of Science and Technology of Oran Mohammed Boudiaf, L.P 1505 EL-Menaour, USTO 31000 Oran, Algeria, E-mail: mbouchetara@hotmail.com

***University of Science and Technology of Oran Mohammed Boudiaf, L.P 1505 EL-Menaour, USTO 31000 Oran, Algeria, E-mail: boutchicha@hotmail.com

 <http://dx.doi.org/10.5755/j01.mech.20.4.6297>

1. Introduction

Clutches or couplings have the task to receive and to transmit power from engine to the driven machine [1]. This is achieved through the transmission of power inside the fluid coupling composed of a centrifugal pump and a turbine [2, 3]. It is often installed as a vibration damping element or as a shock absorber to protect the engine and the driven machine against overloads, for example in vehicles, ships and fixed equipment [4, 5]. Fluid couplings can also act as hydrodynamic brakes, dissipating rotational energy as heat through frictional forces [6]. This type of hydrodynamic transmission is based on the principle of Föttinger [7, 8].

A fluid coupling, sometimes also known as hydraulic coupling or Voith fluid coupling, is a non-mechanical coupling used to transfer the power from a prime mover, an electrical motor or an internal combustion engine, to a driven machine [9].

Simulation of fluid coupling is an important tool for analysing and evaluation of the dynamic behavior of engine - transmission system [10-14]. Torque transmission is possible only if the sliding conditions are ensured [15].

Among the main advantages of hydrodynamic couplings may be mentioned [16-20]:

- in case of overload, the engine cannot stall because of the sliding between the input shaft and the output shaft;
- hydraulic couplers, without being equivalent to torque limiters are safety devices that protect the engine and the driven machine;
- hydrodynamic transmissions are simple in design, easy maintenance; insensitive to wear [21-23].

The main aim of this study is to carry out a numerical simulation of the transient behavior of a hydrodynamic coupling operating in two different modes, start-up and braking.

Through numerical simulation developed, one presents the evolution of the fluid velocity in the coupler and the rotational speed of the primary and secondary shaft, and the variation of the torque of the pump and the turbine as function of time.

To validate the results of the developed numerical simulation model, we realized a test bench that simulates the different operating modes of a hydrodynamic coupling.

2. Fundamental equation of unsteady motion of a hydrodynamic transmission

2.1. Description of the hydrodynamic coupling

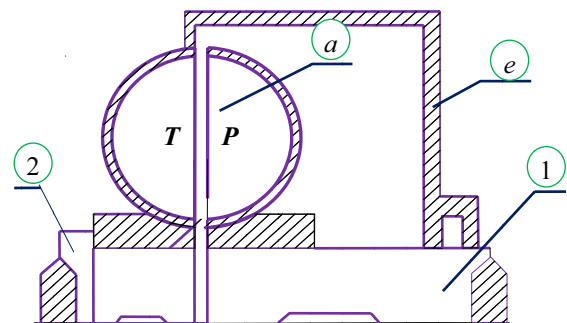


Fig. 1 Schematic representation of a hydrodynamic clutch

The primary shaft *I* linked to an engine that causes the primary rotor *P* by its rotational movement.

Turbine *T* member or secondary rotor which is integral to the tight envelope *e* of the set containing the liquid. Both wheels, the pump *P* and the turbine *T*, are provided with radial blades *a*, Fig. 1.

The torus is the common waterproof body that meets and casing *P* and *T* and replacing the pipes. The oil filling the torus is generally more than 90% of its total capacity to avoid the oil dilution under the influence of heat which can generate excessive pressure on the walls. This phenomenon has caused the explosion of several couplers [24-27].

2.2. Equations of unsteady motion of a hydrodynamic coupling

To establish the basic equations of unsteady motion of a hydrodynamic coupling (Fig. 2), it is assumed that:

- the fluid is incompressible;
- the fluid flows along the median line, because the analysis of the phenomena under microscopic aspects is complicated;
- the flow is along the blade;
- the space between the pump and the turbine is negligible.

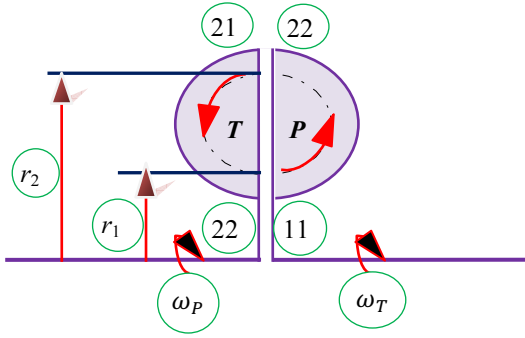


Fig. 2 Schematic of hydrodynamic system in the meridian plan

The mathematical formulation of a torque converter has been developed by Ishihara and Emori Kotwicki, and Hrovat and Tobler [28-30].

The kinetic energy of the total mass of the fluid is:

$$E_c = \int \rho \frac{V^2}{2} AdL, \quad (1)$$

where \int is integral for full closed fluid flow; A is meridian section of the fluid flow, which is perpendicular to the meridian plane.

So the variation of the kinetic energy according to the time is:

$$\left. \begin{aligned} \frac{dE_c}{dt} &= \frac{d}{dt} \int \rho \frac{V^2}{2} AdL = \frac{1}{2} \rho \int \frac{dV^2}{dt} AdL; \\ \frac{dE_c}{dt} &= \rho \int \frac{1}{2} \left(\frac{\partial V^2}{\partial t} + \frac{\partial V^2}{\partial z} \frac{\partial z}{\partial t} \right) AdL, \end{aligned} \right\} \quad (2)$$

where z is length of the average current line.

As $V = \frac{dz}{dt}$ then the relation (2) becomes:

$$\frac{dE_c}{dt} = \rho \int \frac{1}{2} \frac{dV^2}{dz} \frac{dz}{dt} AdL \quad (3)$$

The absolute velocity V is expressed as follows:

$$V^2 = U^2 + C^2; \quad U = r\omega.$$

The integral Eq. (3) becomes:

$$\left. \begin{aligned} \frac{dE_c}{dt} &= \rho \int \frac{1}{2} \frac{d(U^2 + C^2)}{dt} AdL; \\ \frac{dE_c}{dt} &= \rho \left(\int r\omega \frac{d(r\omega)}{dt} AdL + C \frac{dC}{dt} AdL \right); \\ \frac{dE_c}{dt} &= \rho \left(\int r\omega \frac{d(r\omega)}{dt} AdL + Q\Phi \frac{dC_2}{dt} \right), \end{aligned} \right\} \quad (4)$$

with $Q = Ac$ and $\Phi = \int \left(\frac{A_2}{A} \right) dL$; A_2 is meridian section of the fluid flow; C_2 is meridian speed at the entering of turbine.

The moment of the pump is expressed as follows:

$$M_1 = \int_{11}^{12} \frac{\partial (r^2 \omega)}{\partial t} \rho A dL + \rho Q (r_2^2 \omega_1 - r_1^2 \omega_2). \quad (5)$$

The moment of the turbine will be:

$$M_2 = \int_{21}^{22} \frac{\partial (r^2 \omega)}{\partial t} \rho A dL + \rho Q (r_1^2 \omega_2 - r_2^2 \omega_1). \quad (6)$$

The hydraulic power of the pump and the turbine will be respectively:

$$P_1 = \rho \omega_1 \left[\int_{11}^{12} r \frac{\partial (r\omega)}{\partial t} AdL + Q (r_2^2 \omega_1 - r_1^2 \omega_2) \right]; \quad (7)$$

$$P_2 = \rho \omega_2 \left[\int_{21}^{22} r \frac{\partial (r\omega)}{\partial t} AdL - Q (r_2^2 \omega_1 - r_1^2 \omega_2) \right]. \quad (8)$$

During the fluid circulation in the coupling, there are energy losses E_L due to the frictions in the blades, and to the shocks during sudden change of the direction of inlet velocity at the pump and particularly at inlet of the turbine. Energy losses E_L are expressed per unit of time as:

$$\frac{dE_L}{dt} = \frac{1}{2} \rho Q \left[(r_1^2 + r_2^2) (\omega_1 - \omega_2)^2 + LC_2^2 \right], \quad (9)$$

where L is total friction coefficient by full circulation.

The equation of non-steady motion of fluid is obtained by substituting the Eqs. (4), (7)-(9) in the following relationship:

$$\frac{dE_c}{dt} = P_1 + P_2 - \frac{dE_L}{dt}. \quad (10)$$

It follows:

$$\Phi \frac{dC_2}{dt} = \frac{1}{2} \left[(r_2^2 - r_1^2) (\omega_1^2 - \omega_2^2) - LC_2^2 \right]. \quad (11)$$

To obtain the motion equation of the pump, the inertial moment of the pump and of all rotating mechanical parts without the presence of oil, which is denoted J'_1 .

The fluid act on the pump with a reaction time is expressed by Eq. (5).

Equation of motion of the pump:

$$J'_1 \frac{d\omega_1}{dt} = M_P - \rho A_2 c_2 (r_2^2 \omega_1 - r_1^2 \omega_2). \quad (12)$$

Equation of motion of the turbine:

$$J'_2 \frac{d\omega_2}{dt} = \rho A_2 c_2 (r_2^2 \omega_1 - r_1^2 \omega_2) - M_T, \quad (13)$$

J'_1 is inertia moment of the rotating parts of the pump side without the presence of oil; J'_2 is inertia moment of the rotating parts of the turbine side without the presence of oil; ω_1 - angular velocity of the pump wheel; ω_2 is angu-

lar velocity of the turbine wheel; M_p is output torque on the pump; M_T is output torque on the turbine.

By neglecting the inertia moment of the fluid acting on the pump and the turbine, we obtain:

$$J'_1 = J_1 \text{ and } J'_2 = J_2,$$

where J_1 is inertia moment of the pump side with oil, J_2 is inertia moment of the turbine side with oil.

Finally, the motion equations of the pump and the turbine will be respectively:

$$J_1 \frac{d\omega_1}{dt} = M_p - \rho A_2 c_2 (r_2^2 \omega_1 - r_1^2 \omega_2) \quad (14)$$

$$J_2 \frac{d\omega_2}{dt} = \rho A_2 c_2 (r_2^2 \omega_1 - r_1^2 \omega_2) - M_T \quad (15)$$

2.3. Resolution of the equation system

The system of fundamental equations of non-steady movement of the hydrodynamic coupling is written as follows:

$$\begin{cases} \Phi \frac{dc_2}{dt} = \frac{1}{2} [(r_2^2 - r_1^2)(\omega_1^2 - \omega_2^2) - L c_2^2]; \\ J_1 \frac{d\omega_1}{dt} = M_p - \rho A_2 c_2 (r_2^2 \omega_1 - r_1^2 \omega_2); \\ J_2 \frac{d\omega_2}{dt} = \rho A_2 c_2 (r_2^2 \omega_1 - r_1^2 \omega_2) - M_T. \end{cases} \quad (16)$$

We have a system of Eq. (3) to Eq. (5) unknowns, namely: ω_1 is angular velocity of the wheel pumps, rad/s; ω_2 is angular velocity of the wheel turbines, rad/s; c_2 is meridian velocity of the fluid, m/s; M_p is output torque of the pump, daNm; M_T is output torque of the turbine, daNm.

It is more practical to make the system of equations in dimensionless form. The system (16) becomes then:

$$\begin{cases} \frac{dx}{dt_{11}} = \frac{1}{2p} [(1-a^2)(y^2 - z^2) - L x^2]; \\ Q_1 \frac{dy}{dt} = T_1 - x(y - a^2 z); \\ Q_2 \frac{dz}{dt} = x(y - a^2 z) - T_2. \end{cases} \quad (17)$$

$x = \frac{c_2}{r_2 \omega_0}$ is dimensionless speed; ω_0 is engine angular speed; $T_1 = \frac{M_p}{\rho A_2 r_2^3 \omega_0^2}$ is dimensionless moment of the pump wheel; $T_2 = \frac{M_T}{\rho A_2 r_2^3 \omega_0^2}$ is dimensionless moment on the turbine wheel, $Q_1 = \frac{J_1}{\rho A_2 r_2^3}$ is dimensionless moment of inertia of the pump side; $Q_2 = \frac{J_2}{\rho A_2 r_2^3}$ is dimensionless

moment of inertia of the turbine side; $p = \frac{\Phi}{r_2}$ is dimensionless parameter length.

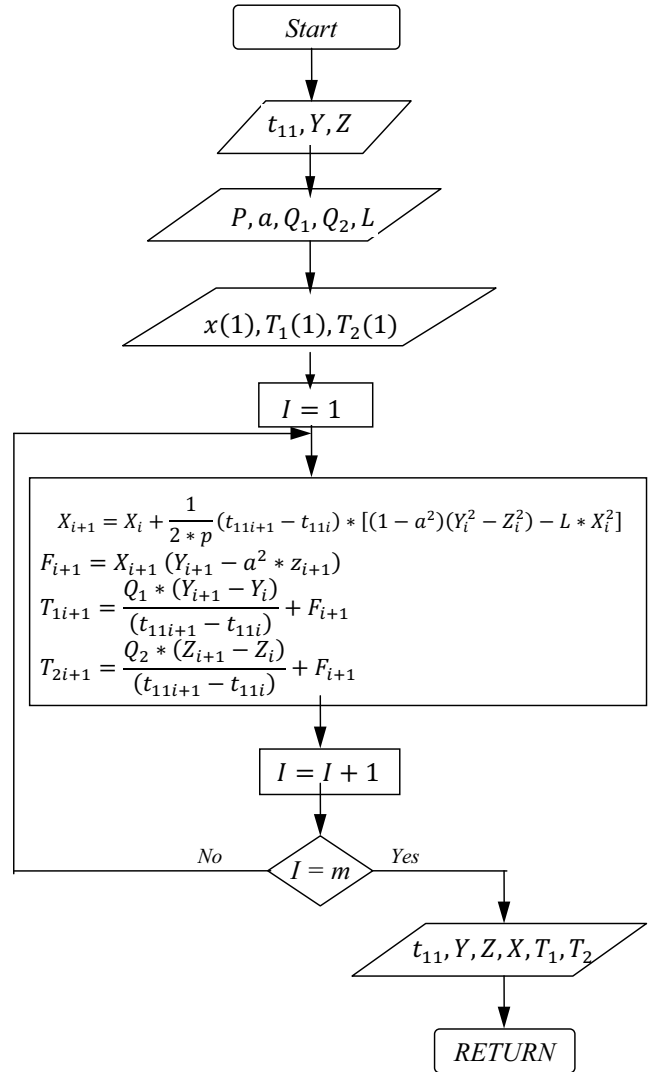


Fig. 3 Flowchart to solving dimensionless equation system

The system (17) becomes then:

$$\begin{cases} \frac{x_{i+1} - x_i}{t_{11i+1} - t_{11i}} = \frac{1}{2p} [(1-a^2)(y^2 - z^2) - L x^2]; \\ T_{1i+1} = Q_1 \frac{y_{i+1} - y_i}{t_{11i+1} - t_{11i}} + x_{i+1} (y_{i+1} - a^2 z_{i+1}); \\ T_{2i+1} = -Q_2 \frac{z_{i+1} - z_i}{t_{11i+1} - t_{11i}} + x_{i+1} (y_{i+1} - a^2 z_{i+1}). \end{cases}$$

$$\begin{cases} x_{i+1} = x_i (t_{11i+1} - t_{11i}) \frac{1}{2p} [(1-a^2)(y_i^2 - z_i^2) - L x_i^2]; \\ F_{i+1} = x_{i+1} (y_{i+1} - a^2 z_{i+1}); \\ T_{1i+1} = Q_1 \frac{y_{i+1} - y_i}{t_{11i+1} - t_{11i}} + F_{i+1}; \\ T_{2i+1} = -Q_2 \frac{z_{i+1} - z_i}{t_{11i+1} - t_{11i}} + F_{i+1}. \end{cases} \quad (18)$$

$t_{11} = \omega_0 t$ is dimensionless time.

It allows solving the system of dimensionless equations (Fig. 3).

3. Description of the test bench of a hydrodynamic clutch

The purpose of this study is to develop a numerical model for simulating the hydraulic coupling operations that allows the analysing of the dynamic behavior of the hydrodynamic coupling, respectively in the starting and braking phase. To validate the elaborated numerical simulation model, we proceed to the realization of a test bench to measure the input and output parameters of a hydrodynamic coupling according to defined operating modes.

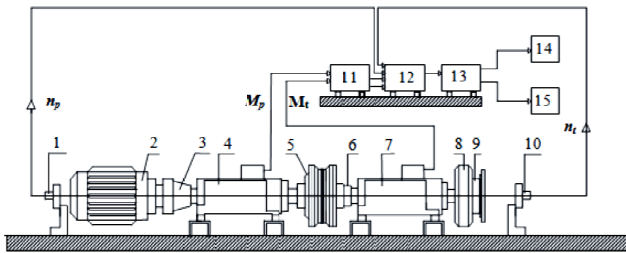


Fig. 4 Plan of the bench test of the hydrodynamic clutch: 1 - tachometer A; 2 - electrical motor; 3 - electromagnetic clutch; 4 - torque measuring device; 5 - hydrodynamic coupling; 6 - rigid coupling; 7 - torque measuring device; 8 - flywheel; 9 - electromagnetic brake; 10 - tachometer; 11 - controller-UNIT-GDI; 12 - recorder (real time analyzer); 13 - Pc ; 14 - plotter; 15 - printer

Table 1

Hydraulic parameters characterizing the hydrodynamic coupling

| | |
|---|------|
| Motor power P_m , kW | 4.00 |
| Nominal rotation speed n_m , rpm | 1436 |
| Specific velocity, n_s | 65 |
| Oil density ρ , kg/m ³ | 800 |
| Number of blades of the pump wheel Z_p | 37 |
| Number of blades of the turbine wheel Z_t | 40 |

Table 2

Technical characteristics of a hydrodynamic coupling

| | Material | Density ρ , kg/m ³ | Total filling capacity V_r , dm ³ | Service capacity V_s , dm ³ |
|---------------------|------------|------------------------------------|--|--|
| Hydrodynamic clutch | Pump | Aluminum alloy | 2.3 | 1.84 |
| | Turbine | Aluminum alloy | | |
| | Torus | Cast iron | | |
| | Lid | Steel | | |
| | Used fluid | Special fluid | | |

On the bench, there are two shafts: the first provides the pump torque and the second the turbine torque. Fig. 4 shows the installation of the used test bench of a hydrodynamic coupling.

Tables 1 and 2 are shown respectively the hydraulic Parameters and the technical characteristics of the tested hydrodynamic coupling.

4. Experimental tests

4.1. Starting tests

Mode 1. Operating steps and test conditions (Fig. 5):

- initially the engine is under normal operating conditions, the turbine is blocked;
- clutch, pump motor, turbine is still blocked;
- unlock the turbine, the pump and the engine under normal operating conditions.

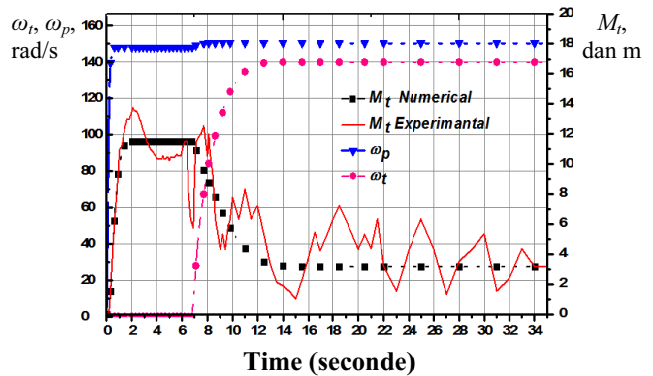


Fig. 5 Test in the starting up - modus operandi -1 -

Mode 2. Operating steps and test conditions (Fig. 6):

- initially engine under normal operating conditions ,the turbine is unlocked;
- clutch, pump-motor, turbine remains unlocked (free).

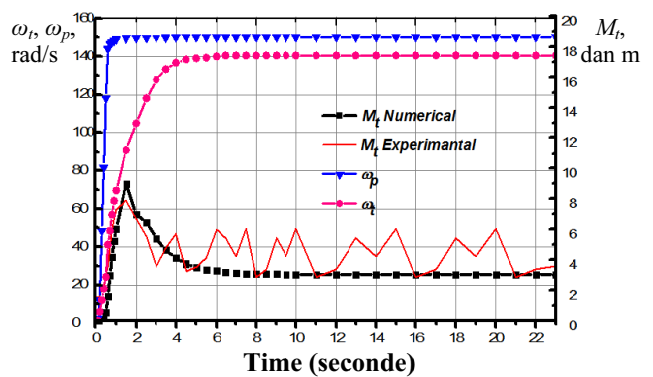


Fig. 6 Test in the starting up - modus operandi - 2 -

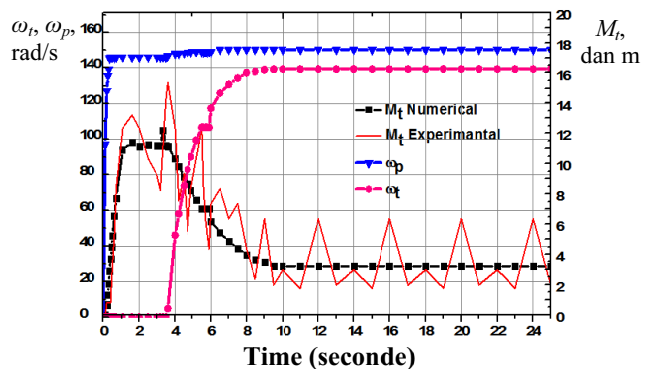


Fig. 7 Test in the starting up - modus operandi - 3 -

Mode 3. Operating steps and test conditions

(Fig. 7):

- initially engine is off and the turbine is blocked;
- let in the clutch;
- motor stopped and turbine is still blocked;
- starting the engine and unlock the turbine.

Mode 4. Operating steps and test conditions

(Fig. 8):

- engine initially on the march normal, and the turbine is freed;
- clutch, turbine is still unlocked and engine at the stop;
- engine is on, the turbine is blocked and the pump running under normal conditions.

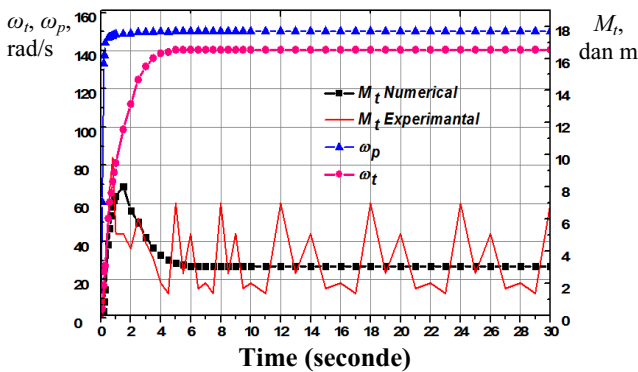


Fig. 8 Test in the starting up - modus operandi - 4 -

4.2. Braking test

Operating steps and test conditions (Fig. 9):

- engine, pump, turbine during normal operation;
- block the turbine engine and pump during normal operation.

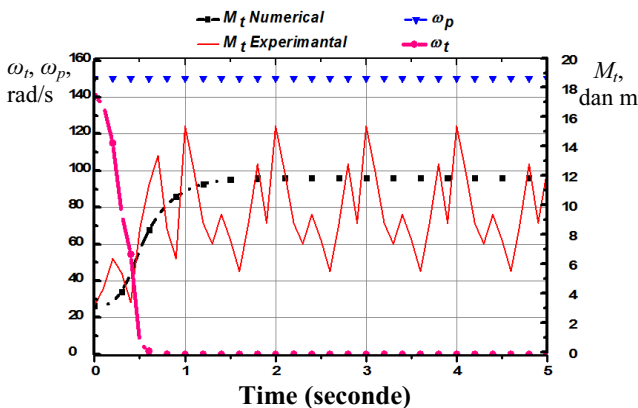


Fig. 9 Test of braking - modus operandi-

5. Analysis and discussion of results

From the Figs. 5-8, the following comments and conclusions can be deduced:

In the modes 1 and 3, the turbine torque M_T evolves into 4 phases: linear increase, stabilization $M_T = \text{constant}$, nearly linear decreasing and until the end of the operation.

The physical interpretation of this curve profile is as follows:

- during the period of blocking, M_T cross from zero to M_{T1} , where M_{T1} is the moment on the turbine wheel and

remains fixed as long as they're blocking;

- just after the releasing, we have noticed the diminution of M_T , this is due to the absence of the resisting moment of blocking;

- in the last phase, the effect of the moments of resisting inertia decreases and thus the moment on the wheel turbines will be equal at the transmitted moment which stays stable regime;

- for modes 2 and 4, the curve of the moment of the turbine wheel M_T evolves in 3 phases to be known: growth in the presence of a peak, decreasing, stabilization.

Even this can be explained as a result:

- the turbine was unlocked (free), the effect of blocking resistance moment is zero, and in this case, the time for the turbine wheel to increase the value of the moment of inertia due to the inertia of the turbine and fluid movement, and later M_T decreases to the normal operating period;

- for braking, it is almost the same as the first phase of start-up (mode 1 and 3), but the difference lies in the initial values ω_p , ω_T , M_T the physical phenomenon is almost the same;

- in the normal operating regime, ω_p , ω_T , M_T have fixed, just after braking (blocking the turbine) ω_T decreases to zero value, while M_T increases and stabilizes at a time equal to the braking torque.

6. Conclusion and future work

1. The developed numerical simulation model represents an efficient tool for analysis and evaluation of the dynamical behavior of hydrodynamic couplings; it can be used to describe the correlation between the input and output main parameters of hydrodynamic transmissions.

2. Due to the increasing use of hydrodynamic transmissions, the present study focused on the analysis of unsteady behavior of hydrodynamic couplings.

3. The numerical simulation developed in this study is based on the elaboration of a system of differential equations describing the unsteady behavior of the hydraulic coupling.

4. To resolve the system of nonlinear differential equations, the method of finite differences was used.

5. The elaborated computing program allows to determine the evolution of speed and torque of the turbine as a function of time by knowing the input parameters of the pump or the engine.

6. The designed test bench has allowed to carry out measurements of the speed and torque on the input and output side of the hydrodynamic coupling as a function of time and imposed operating modes. The experimental and numerical results are almost identical, proving that the test bench and the numerical simulation model were successfully realized.

7. This test bench can be used for other experimental investigations such as the vibration or thermal behavior of hydrodynamic couplings.

References

1. Asl, H.A.; Azad, N.L.; McPhee, J. 2014. Math-based torque converter modelling to evaluate damping characteristics and reverse flow mode operation, International Journal of Vehicle Systems Modelling and Test-

- ing 91: 36-55.
<http://dx.doi.org/10.1504/IJVSMT.2014.059155>.
2. **Lindas, R.** 1988. Embrayages. Etude technologique. Techniques de l'ingénieur. Génie mécanique : B5851.5851- B5851-5822.
 3. **Chapallaz, J.M.; Eichenberger, P.; Fischer, G.** 1992. Manual on Pumps Used as Turbines, 221 p.
 4. **Heisler, H.** 2002. Advanced Vehicle Technology. Access Online via Elsevier, 666 p.
 5. **Vasylius, M.; Didžiokas, R.; Mažeika, P.; Barzdaitis, V.** 2008. The rotating system vibration and diagnostics, *Mechanika* 4: 54-58.
 6. **Bajkowski, J.; Grzesikiewicz, W.** 2001. Matematyczny opisukładów napędowych z uwzględnieniem sił tarcia suchego, *Zeszyty Naukowe, Mechanika/Politechnika Opolska*: 35-50.
 7. **Bärgläzan, M.** 2010. Dynamic Identification of a Hydrodynamic Torque Converter, *UPB Sci. Bull, Series D*, 724.
 8. **Kesy, A.; Kadziela, A.** 2009. Application of statistical formulas to hydrodynamic torque converter modelling, *Archives of Civil and Mechanical Engineering* 94: 33-48.
[http://dx.doi.org/10.1016/S1644-9665\(12\)60067-3](http://dx.doi.org/10.1016/S1644-9665(12)60067-3).
 9. **Zdankus, N.; Kargaudas, V.** 2009. Hydraulic machine wear control by working regime, *Mechanika* 5: 68-73.
 10. **Kolb, A.; Cuntz, N.** 2005. Dynamic particle coupling for GPU-based fluid simulation, In *Proc. Symposium on Simulation Technique*, 722-727.
 11. **Müller, M.; Charypar, D.; Gross, M.** 2003. Particle-based fluid simulation for interactive applications, In *Proceedings of the 2003 ACM SIGGRAPH/ Eurographics symposium on Computer animation*, 154-159, Eurographics Association.
 12. **Batty, C.; Bertails, F.; Bridson, R.** 2007. A fast variational framework for accurate solid-fluid coupling, *ACM Transactions on Graphics TOG*, 26(3).
 13. **Hasegawa, T.; Iida, M.** 1996. U.S. Patent No. 5,542,307. Washington, DC: U.S. Patent and Trademark Office.
 14. **Whitfield, A.; Wallace, F.J.; Patel, A.** 1983. Design of three element hydrokinetic torque converters, *International Journal of Mechanical Sciences* 257: 485-497.
[http://dx.doi.org/10.1016/0020-7403\(83\)90041-3](http://dx.doi.org/10.1016/0020-7403(83)90041-3).
 15. **Krivchenko, G.I.** 1994. *Hydraulic Machines: Turbines and Pumps*, Boca Raton, FL: Lewis publishers, 432 p.
 16. **Robinette, D.; Grimmer, M.; Beikmann, R.** 2011. Dynamic Torque Characteristics of the Hydrodynamic Torque Converter, *SAE International Journal of Passenger Cars-Mechanical Systems* 42: 1023-1032.
 17. **Hellinger, W.** 2004. U.S. Patent No. 6,698,195. Washington, DC: U.S. Patent and Trademark Office.
 18. **Adleff, K.; Höller, H.; Hercher, G.P.; Tietz, M.** 2001. Hydrodynamic coupling, *European Patent No. EP 0801244*. Munich, Germany: European Patent Office.
 19. **Adleff, K.; Hercher, G. P.; Tietz, M.** 2002. *European Patent No. EP 0801243*. Munich, Germany: European Patent Office.
 20. **Lang, T.; Romer, A.; Seeger, J.** 1998. Entwicklungen der Hydraulik in Traktoren und Landmaschinen: Beobachtungen anlässlich der agritechnica'97, *Ölhydraulik und Pneumatik* 422: 87-94.
 21. **Folberth, T.** 2006. Hydrodynamische Kupplung und Antriebseinheit mit einer hydrodynamischen Kupplung.
 22. **Kęsy, A.; Kądziela, A.** 2011. Construction optimization of hydrodynamic torque converter with application of genetic algorithm, *Archives of Civil and Mechanical Engineering* 114: 905-920.
[http://dx.doi.org/10.1016/S1644-9665\(12\)60086-7](http://dx.doi.org/10.1016/S1644-9665(12)60086-7).
 23. **Lindas, R.** 1988. Coupleurs. *Techniques de l'ingénieur*. B5860, B5860-1.
 24. **Lennevi, J.** 1995. Hydrostatic Transmission Control: Design Methodology for Vehicular Drivetrain Applications, PhD thesis, Department of Mechanical Engineering, Linköping University.
 25. **Martelli, M.; Zarotti, L.** 2005. Hydrostatic Transmission with a Traction Control. 2nd ISARC.
 26. **Kesy, A.; Kesy, Z.** 1993. Damping characteristics of a transmission system with a hydrodynamic torque converter, *Journal of Sound and Vibration* 166(3): 493-506.
<http://dx.doi.org/10.1006/jsvi.1993.1308>.
 27. **Grandperrin, G.** 2007. Lignes de courant de fluides incompressibles.
 28. **Ishihara, T. and Emori, R.I.** 1966. Torque converter as a vibrator damper and its transient characteristics, *SAE: Paper 660368*.
 29. **Kotwicki, A.J.** 1982. Dynamic models for torque converter equipped vehicles, *SAE Technical Paper 820393*.
<http://dx.doi.org/10.4271/820393>.
 30. **Hrovat, D.; Tobler, W.E.** 1985. Bond graph modeling and computer simulation of automotive torque converters, *Journal of the Franklin Institute* 319: 93-114.
[http://dx.doi.org/10.1016/0016-0032\(85\)90067-5](http://dx.doi.org/10.1016/0016-0032(85)90067-5).

T. Khatir, M. Bouchetara, D. Boutchicha

HIDRODINAMINĖS JUNGTIŲ EKSPLOATAVIMO EKSPERIMENTINĖ IR SKAITMENINĖ DINAMIKOS ANALIZĖ

R e z i u m ė

Hidrodinaminė sankaba yra sujungimo įrenginys veikiantis hidrodinaminės transmisijos principu. Ji funkcionuoja hidrodinamikos principu. Hidrodinaminė sankaba susideda iš siurblio (dažnai vadinamos sparnuote) ir turbiną vadinamos rotoriumi, abi dalys apjungiant gaubtu. Toks hidrodinaminis įrenginys naudojamas perduodant sukamąjį judesį. Šiam sujungimui būdingos centrifūgos savybės paleidimo metu. Tai užtikrina variklio paleidimą be apkrovos, kas yra labai svarbu. Toks sujungimas naudojamas automobilinėse transmisijose pakeičiant mechaninę sankabą. Straipsnyje aprašomas hidrodinaminis jungčių arba sankabų bandymo standas, kuriame tiriama jungiamosios movos nenusistovėjęs režimas. Atliktas šio reiškinio teorinis tyrimas pagrįstas siurblio bei turbinos ratų ir skysčio judėjimo lygčių sistemos sprendimu. Skaitmeninei analizei parašyta specialia Fortran 90 programa skirta greičių ir momentų nustatymui. Gauti rezultatai palyginti su eksperimentiniais ir pateikti grafikų pavidalu.

T. Khatir, M. Bouchetara, D. Boutchicha

DYNAMICS STUDY OF THE OPERATING
BEHAVIOR OF HYDRODYNAMIC COUPLING BY
EXPERIMENTAL AND NUMERICAL SIMULATION

S u m m a r y

The hydrodynamic clutch is a device of coupling which works according to the principle of the hydrodynamic transmission. Fluid couplings work on the hydrodynamic principle. It consists of a pump-generally known as impeller and a turbine generally known as rotor, both enclosed suitably in a casing. It is a hydrodynamic device used to transmit rotating mechanical power. The Fluid coupling has centrifugal characteristics during starting, thus enabling no load start-up of prime mover, which is of great importance. It has been used in automobile transmissions as an alternative to a mechanical clutch. This study

aimed at the installation of a test bench of hydrodynamic couplings or clutches, on which it was planned to, analyze the pressing problems of the coupler in its not still regime. One parallel in the experimental part, we made a theoretical study of these phenomena which based itself essentially on the resolution of a system of equations of movement of the wheel-pump, the wheel-turbine and the fluid. For the numerical simulation, a special program is written in FORTRAN 90 were used, we'll find the values of characteristic of speed and the moments, we compared the two results. They are given in the form of the curves.

Keywords: clutch, hydrodynamic coupling, numerical simulation, coupler, wheel-pump, wheel-turbine, hydrodynamic transmission, fluid coupling.

Received January 28, 2014

Accepted June 18, 2014